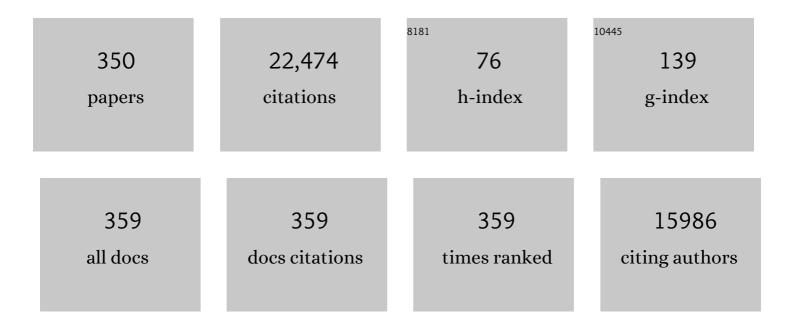
## Junko N Kondo

List of Publications by Year in descending order

Source: https://exaly.com/author-pdf/6195168/publications.pdf Version: 2024-02-01



#	Article	IF	CITATIONS
1	Conduction and Valence Band Positions of Ta2O5, TaON, and Ta3N5by UPS and Electrochemical Methods. Journal of Physical Chemistry B, 2003, 107, 1798-1803.	2.6	917
2	Oxysulfide Sm2Ti2S2O5as a Stable Photocatalyst for Water Oxidation and Reduction under Visible Light Irradiation (λ ≤50 nm). Journal of the American Chemical Society, 2002, 124, 13547-13553.	13.7	890
3	Cu2O as a photocatalyst for overall water splitting under visible light irradiation. Chemical Communications, 1998, , 357-358.	4.1	747
4	Biodiesel made with sugar catalyst. Nature, 2005, 438, 178-178.	27.8	735
5	An oxynitride, TaON, as an efficient water oxidation photocatalyst under visible light irradiation (λ â‰₱Tj ETQq1	1 0,78431 4.1	4.rgBT /Ove
6	A Carbon Material as a Strong Protonic Acid. Angewandte Chemie - International Edition, 2004, 43, 2955-2958.	13.8	519
7	Acid-Catalyzed Reactions on Flexible Polycyclic Aromatic Carbon in Amorphous Carbon. Chemistry of Materials, 2006, 18, 3039-3045.	6.7	509
8	Nb <sub>2</sub> O <sub>5</sub> ·nH <sub>2</sub> O as a Heterogeneous Catalyst with Water-Tolerant Lewis Acid Sites. Journal of the American Chemical Society, 2011, 133, 4224-4227.	13.7	480
9	Photoreactions on LaTiO2N under Visible Light Irradiation. Journal of Physical Chemistry A, 2002, 106, 6750-6753.	2.5	443
10	RuO2-Loaded β-Ge3N4as a Non-Oxide Photocatalyst for Overall Water Splitting. Journal of the American Chemical Society, 2005, 127, 4150-4151.	13.7	388
11	Ta3N5as a Novel Visible Light-Driven Photocatalyst (λ<600 nm). Chemistry Letters, 2002, 31, 736-737.	1.3	377
12	Photocatalytic Decomposition of Water on Spontaneously Hydrated Layered Perovskites. Chemistry of Materials, 1997, 9, 1063-1064.	6.7	351
13	TaON and Ta3N5 as new visible light driven photocatalysts. Catalysis Today, 2003, 78, 555-560.	4.4	339
14	Photo- and Mechano-Catalytic Overall Water Splitting Reactions to Form Hydrogen and Oxygen on Heterogeneous Catalysts. Bulletin of the Chemical Society of Japan, 2000, 73, 1307-1331.	3.2	316
15	LaTiO2N as a Visible-Light (â‰ <b>ø</b> 00 nm)-Driven Photocatalyst (2). Journal of Physical Chemistry B, 2003, 107, 791-797.	2.6	288
16	Selective Hydrogenation of Acetylene over Au/Al2O3Catalyst. Journal of Physical Chemistry B, 2000, 104, 11153-11156.	2.6	281
17	Esterification of higher fatty acids by a novel strong solid acid. Catalysis Today, 2006, 116, 157-161.	4.4	266
18	Exfoliated Nanosheets as a New Strong Solid Acid Catalyst. Journal of the American Chemical Society, 2003, 125, 5479-5485.	13.7	247

#	Article	IF	CITATIONS
19	Recent progress of photocatalysts for overall water splitting. Catalysis Today, 1998, 44, 17-26.	4.4	230
20	Mesoporous Tantalum Oxide. 1. Characterization and Photocatalytic Activity for the Overall Water Decomposition. Chemistry of Materials, 2001, 13, 1194-1199.	6.7	229
21	Control of the Al Distribution in the Framework of ZSM-5 Zeolite and Its Evaluation by Solid-State NMR Technique and Catalytic Properties. Journal of Physical Chemistry C, 2015, 119, 15303-15315.	3.1	227
22	Visible light-induced photocatalytic behavior of a layered perovskite-type rubidium lead niobate, RbPb2Nb3O10. The Journal of Physical Chemistry, 1993, 97, 1970-1973.	2.9	216
23	A highly active photocatalyst for overall water splitting with a hydrated layered perovskite structure. Journal of Photochemistry and Photobiology A: Chemistry, 1997, 106, 45-49.	3.9	204
24	Crystallization of Mesoporous Metal Oxides. Chemistry of Materials, 2008, 20, 835-847.	6.7	198
25	Recent progress of visible-light-driven heterogeneous photocatalysts for overall water splitting. Solid State Ionics, 2004, 172, 591-595.	2.7	194
26	Heterogeneous Ni Catalyst for Direct Synthesis of Primary Amines from Alcohols and Ammonia. ACS Catalysis, 2013, 3, 112-117.	11.2	185
27	Oxysulfides Ln2Ti2S2O5as Stable Photocatalysts for Water Oxidation and Reduction under Visible-Light Irradiation. Journal of Physical Chemistry B, 2004, 108, 2637-2642.	2.6	169
28	Unusual enhancement of H2 evolution by Ru on TaON photocatalyst under visible light irradiation. Chemical Communications, 2003, , 3000.	4.1	166
29	Facile control of crystallite size of ZSM-5 catalyst for cracking of hexane. Microporous and Mesoporous Materials, 2011, 145, 165-171.	4.4	163
30	Effect of desilication of H-ZSM-5 by alkali treatment on catalytic performance in hexane cracking. Applied Catalysis A: General, 2012, 449, 188-197.	4.3	163
31	Synthesis of Crystallized Mesoporous Tantalum Oxide and Its Photocatalytic Activity for Overall Water Splitting under Ultraviolet Light Irradiation. Chemistry of Materials, 2008, 20, 5361-5367.	6.7	162
32	Preparation of K2La2Ti3O10by Polymerized Complex Method and Photocatalytic Decomposition of Water. Chemistry of Materials, 1998, 10, 72-77.	6.7	161
33	Protonated Titanate Nanotubes as Solid Acid Catalyst. Journal of the American Chemical Society, 2010, 132, 6622-6623.	13.7	159
34	A Stable and Highly Active Hybrid Mesoporous Solid Acid Catalyst. Advanced Materials, 2005, 17, 1839-1842.	21.0	151
35	Electrochemical Behavior of Thin Ta3N5Semiconductor Film. Journal of Physical Chemistry B, 2004, 108, 11049-11053.	2.6	146
36	FT-IR studies of the interaction between zeolitic hydroxyl groups and small molecules. 1. Adsorption of nitrogen on H-mordenite at low temperature. The Journal of Physical Chemistry, 1993, 97, 10761-10768.	2.9	140

#	Article	IF	CITATIONS
37	Mechano-catalytic overall water splitting. Chemical Communications, 1998, , 2185-2186.	4.1	139
38	Amorphous Carbon Bearing Sulfonic Acid Groups in Mesoporous Silica as a Selective Catalyst. Chemistry of Materials, 2009, 21, 186-193.	6.7	136
39	Dealuminated Beta zeolite as effective bifunctional catalyst for direct transformation of glucose to 5-hydroxymethylfurfural. Applied Catalysis A: General, 2014, 470, 318-326.	4.3	135
40	Al distribution and catalytic performance of ZSM-5 zeolites synthesized with various alcohols. Journal of Catalysis, 2017, 353, 1-10.	6.2	134
41	Infrared studies of adsorbed species of H2, CO and CO2 over ZrO2. Journal of the Chemical Society Faraday Transactions I, 1988, 84, 511.	1.0	133
42	TiNxOyFzas a Stable Photocatalyst for Water Oxidation in Visible Light (<570 nm). Chemistry Letters, 2003, 32, 196-197.	1.3	133
43	The study of methanol-to-olefin over proton type aluminosilicate CHA zeolites. Microporous and Mesoporous Materials, 2008, 112, 153-161.	4.4	129
44	Highly Active Mesoporous Nb–W Oxide Solidâ€Acid Catalyst. Angewandte Chemie - International Edition, 2010, 49, 1128-1132.	13.8	124
45	Preparation of Porous Niobium Oxides by Soft-Chemical Process and Their Photocatalytic Activity. Chemistry of Materials, 1997, 9, 2179-2184.	6.7	121
46	Variability in the Structure of Supported MoO3 Catalysts:  Studies Using Raman and X-ray Absorption Spectroscopy with ab Initio Calculations. Journal of Physical Chemistry B, 2001, 105, 8519-8530.	2.6	121
47	Ta3N5and TaON Thin Films on Ta Foil:Â Surface Composition and Stability. Journal of Physical Chemistry B, 2003, 107, 13441-13445.	2.6	121
48	Three-Dimensionally Ordered Mesoporous Niobium Oxide. Journal of the American Chemical Society, 2002, 124, 11256-11257.	13.7	120
49	Photocatalytic Decomposition of Acetaldehyde under Visible Light Irradiation over La3+and N Co-doped TiO2. Chemistry Letters, 2003, 32, 1156-1157.	1.3	118
50	Exfoliated HNb3O8Nanosheets as a Strong Protonic Solid Acid. Chemistry of Materials, 2005, 17, 2487-2489.	6.7	117
51	Synthesis and analysis of CO2 adsorbents based on cerium oxide. Journal of CO2 Utilization, 2014, 8, 34-38.	6.8	109
52	Selective oxidation of alcohols to aldehydes/ketones over copper oxide-supported gold catalysts. Journal of Catalysis, 2013, 299, 10-19.	6.2	107
53	An Ethoxy Intermediate in Ethanol Dehydration on BrÃ,nsted Acid Sites in Zeolite. Journal of Physical Chemistry B, 2005, 109, 10969-10972.	2.6	106
54	Photocatalytic reduction of water by TaON under visible light irradiation. Catalysis Today, 2004, 90, 313-317.	4.4	103

#	Article	IF	CITATIONS
55	Catalytic application of sulfonic acid functionalized mesoporous benzene–silica with crystal-like pore wall structure in esterification. Journal of Molecular Catalysis A, 2005, 230, 85-89.	4.8	103
56	Facile Fabrication of ZSM-5 Zeolite Catalyst with High Durability to Coke Formation during Catalytic Cracking of Paraffins. ACS Catalysis, 2013, 3, 74-78.	11.2	103
57	Preparation of Silica Pillared Ca2Nb3O10 and Its Photocatalytic Activity. Chemistry of Materials, 1996, 8, 2534-2538.	6.7	101
58	Titanium Niobate and Titanium Tantalate Nanosheets as Strong Solid Acid Catalysts. Journal of Physical Chemistry B, 2004, 108, 11549-11555.	2.6	99
59	Infrared study of hydrogen adsorbed on ZrO2. Journal of the Chemical Society, Faraday Transactions, 1990, 86, 397.	1.7	97
60	Mechano-catalysis—a novel method for overall water splitting. Physical Chemistry Chemical Physics, 1999, 1, 4485-4491.	2.8	94
61	A comparative IR characterization of acidic sites on HY zeolite by pyridine and CO probes with silica–alumina and γ-alumina references. Physical Chemistry Chemical Physics, 2010, 12, 11576.	2.8	93
62	Effect of Chromium Addition for Photocatalytic Overall Water Splitting on Ni–K2La2Ti3O10. Journal of Catalysis, 2000, 196, 362-365.	6.2	92
63	Novel Synthesis and Photocatalytic Activity of Oxysulfide Sm2Ti2S2O5. Chemistry of Materials, 2003, 15, 4442-4446.	6.7	92
64	Porous Single-Crystalline TaON and Ta3N5 Particles. Chemistry of Materials, 2004, 16, 1603-1605.	6.7	92
65	FT-IR Study of H218O Adsorption on H-ZSM-5:Â Direct Evidence for the Hydrogen-Bonded Adsorption of Water. The Journal of Physical Chemistry, 1996, 100, 1442-1444.	2.9	91
66	Effect of the particle size for photocatalytic decomposition of water on Ni-loaded K4Nb6O17. Microporous Materials, 1997, 9, 253-258.	1.6	91
67	Evidence for a "Carbeneâ€likeâ€Intermediate during the Reaction of Methoxy Species with Light Alkenes on Hâ€ZSMâ€5. Angewandte Chemie - International Edition, 2011, 50, 1853-1856.	13.8	91
68	Direct Comparison of N2 and CO as IR-Spectroscopic Probes of Acid Sites in H-ZSM-5 Zeolite. The Journal of Physical Chemistry, 1995, 99, 10573-10580.	2.9	90
69	Crystallization of an Ordered Mesoporous Nb–Ta Oxide. Angewandte Chemie - International Edition, 2003, 42, 2382-2385.	13.8	90
70	A Comparative Study of Methanol to Olefin over CHA and MTF Zeolites. Journal of Physical Chemistry C, 2007, 111, 5409-5415.	3.1	90
71	Synthesis of Mesoporous Silica Nanospheres Promoted by Basic Amino Acids and their Catalytic Application. Chemistry of Materials, 2010, 22, 3900-3908.	6.7	88
72	Visible-light-driven photocatalytic behavior of tantalum-oxynitride and nitride. Research on Chemical Intermediates, 2007, 33, 13-25.	2.7	86

#	Article	IF	CITATIONS
73	Layered niobium oxides pillaring and exfoliation. Catalysis Today, 1996, 28, 167-174.	4.4	85
74	Structure and Acid Catalysis of Mesoporous Nb <sub>2</sub> O <sub>5</sub> Â <i>n</i> H <sub>2</sub> O. Chemistry of Materials, 2010, 22, 3332-3339.	6.7	82
75	Dehydration of xylose over sulfated tin oxide catalyst: Influences of the preparation conditions on the structural properties and catalytic performance. Applied Catalysis A: General, 2011, 408, 117-124.	4.3	82
76	Ethane-bridged hybrid mesoporous functionalized organosilicas with terminal sulfonic groups and their catalytic applications. Journal of Materials Chemistry, 2005, 15, 666.	6.7	80
77	Heterogeneous cobalt catalysts for the acceptorless dehydrogenation of alcohols. Green Chemistry, 2013, 15, 418-424.	9.0	78
78	Metal ion and N co-doped TiO2 as a visible-light photocatalyst. Journal of Materials Research, 2004, 19, 2100-2108.	2.6	77
79	Partial oxidation of methane to syngas over promoted C12A7. Applied Catalysis A: General, 2004, 277, 239-246.	4.3	77
80	Direct Production of Propene from Methoxy Species and Dimethyl Ether over H-ZSM-5. Journal of Physical Chemistry C, 2012, 116, 24091-24097.	3.1	76
81	(Oxy)nitrides as New Photocatalysts for Water Splitting under Visible Light Irradiation. Electrochemistry, 2002, 70, 463-465.	1.4	74
82	Single-Crystal Particles of Mesoporous Niobiumâ^'Tantalum Mixed Oxide. Chemistry of Materials, 2002, 14, 867-875.	6.7	73
83	New aspects of heterogeneous photocatalysts for water decomposition. Korean Journal of Chemical Engineering, 2001, 18, 862-866.	2.7	71
84	Low temperature CO pulse adsorption for the determination of Pt particle size in a Pt/cerium-based oxide catalyst. Applied Catalysis A: General, 2009, 370, 108-113.	4.3	70
85	Preparation of Crystallized Mesoporous Ta <sub>3</sub> N <sub>5</sub> Assisted by Chemical Vapor Deposition of Tetramethyl Orthosilicate. Chemistry of Materials, 2010, 22, 3854-3861.	6.7	70
86	Formation and Desorption of Oxygen Species in Nanoporous Crystal 12CaO·7Al2O3. Chemistry of Materials, 2004, 16, 104-110.	6.7	68
87	Control of Al Distribution in the CHA-Type Aluminosilicate Zeolites and Its Impact on the Hydrothermal Stability and Catalytic Properties. Industrial & Engineering Chemistry Research, 2018, 57, 3914-3922.	3.7	67
88	Low-temperature methanol dehydration to dimethyl ether over various small-pore zeolites. Applied Catalysis B: Environmental, 2017, 217, 247-255.	20.2	65
89	Construction of Fe2O3 loaded and mesopore confined thin-layer titania catalyst for efficient NH3-SCR of NOx with enhanced H2O/SO2 tolerance. Applied Catalysis B: Environmental, 2021, 287, 119982.	20.2	64
90	Ultrafast Encapsulation of Metal Nanoclusters into MFI Zeolite in the Course of Its Crystallization: Catalytic Application for Propane Dehydrogenation. Angewandte Chemie - International Edition, 2020, 59, 19669-19674.	13.8	63

#	Article	IF	CITATIONS
91	In-Situ Observation of Hydrogenation of Ethylene on a Pt(111) Surface under Atmospheric Pressure by Infrared Reflection Absorption Spectroscopy. Journal of Physical Chemistry B, 1999, 103, 4562-4565.	2.6	62
92	Synthesis, Mesostructure, and Photocatalysis of a Highly Ordered and Thermally Stable Mesoporous Mg and Ta Mixed Oxide. Chemistry of Materials, 2004, 16, 4304-4310.	6.7	62
93	Stable Dimerized Alkoxy Species of 2-Methylpropene on Mordenite Zeolite Studied by FT-IR. Journal of Physical Chemistry B, 1999, 103, 5681-5686.	2.6	61
94	Preparation of Thin Films of a Layered Titanate by the Exfoliation of CsxTi(2-x/4)x/4O4. Chemistry of Materials, 1998, 10, 329-333.	6.7	60
95	Acid Property of Silanol Groups on Zeolites Assessed by Reaction Probe IR Study. Journal of Catalysis, 2000, 191, 275-281.	6.2	59
96	Detailed Process of Adsorption of Alkanes and Alkenes on Zeolites. Journal of Physical Chemistry B, 2005, 109, 1464-1472.	2.6	59
97	Synthesis and Characterization of Mesoporous Taâ^'W Oxides as Strong Solid Acid Catalysts. Chemistry of Materials, 2010, 22, 3072-3078.	6.7	59
98	Ion-exchangeable layered niobates as photocatalysts. Catalysis Today, 1993, 16, 479-486.	4.4	58
99	Preparation of porous niobium oxide by the exfoliation of K <sub>4</sub> Nb <sub>6</sub> O <sub>17</sub> and its photocatalytic activity. Journal of Materials Research, 1998, 13, 861-865.	2.6	58
100	Preparation of a high active photocatalyst, K <sub>2</sub> La <sub>2</sub> Ti <sub>3</sub> O <sub>10</sub> , by polymerized complex method and its photocatalytic activity of water splitting. Journal of Materials Research, 1998, 13, 852-855.	2.6	55
101	Differences in Al distribution and acidic properties between RTH-type zeolites synthesized with OSDAs and without OSDAs. Physical Chemistry Chemical Physics, 2014, 16, 4155.	2.8	55
102	Single crystal particles of a mesoporous mixed transition metal oxide with a wormhole structure. Chemical Communications, 2001, , 2118-2119.	4.1	54
103	Preparation and crystallization characteristics of mesoporous TiO2 and mixed oxides. Journal of Materials Chemistry, 2005, 15, 2035.	6.7	53
104	Preparation and Characterization of Sodium Tantalate Thin Films by Hydrothermalâ^'Electrochemical Synthesis. Chemistry of Materials, 2005, 17, 2422-2426.	6.7	53
105	Preparation of a colloidal array of NaTaO3 nanoparticles via a confined space synthesis route and its photocatalytic application. Physical Chemistry Chemical Physics, 2011, 13, 2563.	2.8	52
106	FT-IR Studies of the Interaction between Zeolitic Hydroxyl Groups and Small Molecules. 3. Adsorption of Oxygen, Argon, Nitrogen, and Xenon on Hâ^'ZSM-5 at Low Temperaturesâ€. The Journal of Physical Chemistry, 1996, 100, 4154-4159.	2.9	51
107	Preparation of Ion-Exchangeable Thin Films of Layered Niobate K4Nb6O17. Chemistry of Materials, 1998, 10, 1647-1651.	6.7	51
108	IR observation of adsorption and reactions of olefins on H-form zeolites. Journal of Molecular Catalysis A, 2003, 199, 27-38.	4.8	51

#	Article	IF	CITATIONS
109	IR Study of H2O Adsorbed on H-ZSM-5. Langmuir, 1997, 13, 747-750.	3.5	50
110	Catalytic cracking of n-hexane for producing propylene on MCM-22 zeolites. Applied Catalysis A: General, 2015, 504, 192-202.	4.3	50
111	DoubleBond Migration of an Olefin without Protonated Species on H(D) Form Zeolites. Journal of Physical Chemistry B, 1997, 101, 9314-9320.	2.6	49
112	A Study of Mechano-Catalysts for Overall Water Splitting. Journal of Physical Chemistry B, 2000, 104, 780-785.	2.6	49
113	Control of Reactivity in Câ^'H Bond Breaking Reactions on Oxide Catalysts:Â Methanol Oxidation on Supported Molybdenum Oxide. Journal of Physical Chemistry B, 2003, 107, 1845-1852.	2.6	48
114	Extremely Stable Zeolites Developed via Designed Liquid-Mediated Treatment. Journal of the American Chemical Society, 2020, 142, 3931-3938.	13.7	48
115	IR Study of Adsorption of Olefins on Deuterated ZSM-5. Journal of Physical Chemistry B, 1998, 102, 2259-2262.	2.6	47
116	Development of highly active SO3H-modified hybrid mesoporous catalyst. Catalysis Today, 2006, 116, 151-156.	4.4	47
117	Activation of hydrocarbons on acidic zeolites: superior selectivity of methylation of ethene with methanol to propene on weakly acidic catalysts. Chemical Communications, 2008, , 5164.	4.1	47
118	Acidic and catalytic properties of ZSM-5 zeolites with different Al distributions. Catalysis Today, 2018, 303, 64-70.	4.4	46
119	Selective oxidation of methane to methanol with H <sub>2</sub> O <sub>2</sub> over an Fe-MFI zeolite catalyst using sulfolane solvent. Chemical Communications, 2019, 55, 2896-2899.	4.1	46
120	IR study of adsorption and reaction of 1-butene on H-ZSM-5. Catalysis Letters, 1997, 47, 129-133.	2.6	45
121	Mechano-catalytic overall water splitting (II) nafion-deposited Cu2O. Applied Catalysis A: General, 2000, 190, 35-42.	4.3	45
122	Ï€-bonded ethene on Pt(111) surface studied by IRAS. Surface Science, 1996, 357-358, 634-638.	1.9	44
123	Reversibly Adsorbed π-Bonded Ethene on Pt(111) Surfaces by Infrared Reflection Absorption Spectroscopy. Langmuir, 1996, 12, 1926-1927.	3.5	44
124	Synthesis of 2D-hexagonally ordered mesoporous niobium and tantalum mixed oxide. Journal of Materials Chemistry, 2002, 12, 1480-1483.	6.7	44
125	Site Conversion of Methoxy Species on ZrO2. Journal of Physical Chemistry B, 1997, 101, 4867-4869.	2.6	43
126	Structure of Dimerized Alkoxy Species of 2-Methylpropene on Zeolites and Silicaâ^'Alumina Studied by FT-IR. Journal of Physical Chemistry B, 1999, 103, 8538-8543.	2.6	43

#	Article	IF	CITATIONS
127	FT-IR study of the interaction of oxygen, argon, helium, nitrogen and xenon with hydroxyl groups in H-Y zeolite at low temperatures. Microporous Materials, 1997, 8, 29-37.	1.6	42
128	Mesoporous Ta Oxide. 2. Improvement of the Synthetic Method and Observation of Mesostructure Formation. Chemistry of Materials, 2001, 13, 1200-1206.	6.7	42
129	Hydrogenated Borophene Shows Catalytic Activity as Solid Acid. ACS Omega, 2019, 4, 14100-14104.	3.5	42
130	Synthesis of graphene mesosponge <i>via</i> catalytic methane decomposition on magnesium oxide. Journal of Materials Chemistry A, 2021, 9, 14296-14308.	10.3	42
131	Perovskite-type La2Ti2O7 mesoporous photocatalyst. Journal of Solid State Chemistry, 2012, 192, 87-92.	2.9	41
132	Formation of alkenyl carbenium ions by adsorption of cyclic precursors on zeolites. Catalysis Today, 2002, 73, 113-125.	4.4	40
133	An anion-conductive microporous membrane composed of a rigid ladder polymer with a spirobiindane backbone. Journal of Materials Chemistry A, 2016, 4, 17655-17659.	10.3	40
134	In situ infrared study of n-heptane isomerization over Pt/H-beta zeolites. Journal of Catalysis, 2007, 248, 53-59.	6.2	38
135	The influence of acidities of boron- and aluminium-containing MFI zeolites on co-reaction of methanol and ethene. Physical Chemistry Chemical Physics, 2011, 13, 14598.	2.8	38
136	IR Characterization of Homogeneously Mixed Silica–Alumina Samples and Dealuminated Y Zeolites by Using Pyridine, CO, and Propene Probe Molecules. Journal of Physical Chemistry C, 2013, 117, 14043-14050.	3.1	38
137	Mechano-catalytic overall water splitting on some mixed oxides. Catalysis Today, 2000, 63, 175-181.	4.4	37
138	Oxidative Dehydrogenation of Propane with CO2 Over Cr/H[B]MFI Catalysts. Catalysis Letters, 2011, 141, 670-677.	2.6	37
139	Highâ€Performance Titanosilicate Catalyst Obtained through Combination of Liquidâ€Phase and Solidâ€Phase Transformation Mechanisms. ChemCatChem, 2014, 6, 2719-2726.	3.7	37
140	Improvement of catalytic performance of MCM-22 in the cracking of n-hexane by controlling the acidic property. Journal of Catalysis, 2016, 333, 17-28.	6.2	37
141	Title is missing!. Catalysis Letters, 1999, 59, 51-54.	2.6	36
142	Synthesis of Highly Ordered Hybrid Mesoporous Material Containing Etenylene (–CH=CH–) within the Silicate Framework. Chemistry Letters, 2003, 32, 950-951.	1.3	36
143	FT-IR Studies of Interaction between Zeolitic Hydroxyl Groups and Small Molecules. 2. Adsorption of Oxygen, Hydrogen, and Rare Gases on H-Mordenite at Low Temperatures. The Journal of Physical Chemistry, 1995, 99, 14805-14812.	2.9	35
144	IR study of reaction of 2â€butene adsorbed on deuterated ZSMâ€5 and mordenite. Catalysis Letters, 1998, 53, 215-220.	2.6	35

#	Article	IF	CITATIONS
145	Improvement in the catalytic properties of ZSM-5 zeolite nanoparticles via mechanochemical and chemical modifications. Catalysis Science and Technology, 2016, 6, 2598-2604.	4.1	35
146	Infrared Investigation of Dynamic Behavior of BrÃ,nsted Acid Sites on Zeolites at High Temperatures. Journal of Physical Chemistry C, 2017, 121, 25411-25420.	3.1	35
147	Mechano-catalytic overall water-splitting into hydrogen and oxygen on some metal oxides. Applied Energy, 2000, 67, 159-179.	10.1	34
148	Synthesis, characterization, and catalytic properties of H-Al-YNU-1 and H-Al-MWW with different Si/Al ratios. Journal of Catalysis, 2009, 266, 268-278.	6.2	34
149	Infrared study of molecularly adsorbed H2 on ZrO2. Chemical Physics Letters, 1992, 188, 443-445.	2.6	33
150	IRAS Studies of Adsorbed Ethene (C2H4) on Clean and Oxygen-Covered Cu(110) Surfaces. The Journal of Physical Chemistry, 1994, 98, 7653-7656.	2.9	33
151	Preparation of a SiO2-Pillared K0.8Fe0.8Ti1.2O4 and IR Study of N2 Adsorption. The Journal of Physical Chemistry, 1995, 99, 16043-16046.	2.9	33
152	Activation Energies for the Reaction of Ethoxy Species to Ethene over Zeolites. Journal of Physical Chemistry C, 2010, 114, 20107-20113.	3.1	33
153	Visible Light Induced Hydrogen Evolution on CdS/K4Nb6O17Photocatalyst. Bulletin of the Chemical Society of Japan, 1995, 68, 2439-2445.	3.2	32
154	FT-IR and Quantum Chemical Studies of the Interaction between Dimethyl Ether and HZSM-5 Zeolite. The Journal of Physical Chemistry, 1996, 100, 11649-11653.	2.9	32
155	Hydrogen Adsorption on Ru/ZrO2Studied by FT-IR. Journal of Physical Chemistry B, 1999, 103, 3229-3234.	2.6	32
156	Reactive and Inert Surface Species Observed during Methanol Oxidation over Silica-Supported Molybdenum Oxide. Journal of Physical Chemistry B, 2002, 106, 12965-12977.	2.6	32
157	Catalytic Activities of Alcohol Transformations Over 8-Ring Zeolites. Topics in Catalysis, 2009, 52, 1272-1280.	2.8	32
158	Proton conduction in alkali metal ion-exchanged porous ionic crystals. Physical Chemistry Chemical Physics, 2017, 19, 29077-29083.	2.8	32
159	Rigid-to-Flexible Conformational Transformation: An Efficient Route to Ring-Opening of a Tröger's Base-Containing Ladder Polymer. ACS Macro Letters, 2017, 6, 775-780.	4.8	32
160	Catalytic dehydration of ethanol-to-ethylene over Rho zeolite under mild reaction conditions. Microporous and Mesoporous Materials, 2019, 282, 91-99.	4.4	32
161	Infrared Study of Hydrogenation of Benzoic Acid to Benzaldehyde on ZrO2Catalysts. Bulletin of the Chemical Society of Japan, 1993, 66, 3085-3090.	3.2	31
162	IR Observation of Selective Oxidation of Cyclohexene with H <sub>2</sub> O <sub>2</sub> over Mesoporous Nb <sub>2</sub> O <sub>5</sub> . Journal of Physical Chemistry C, 2009, 113, 21693-21699.	3.1	31

#	Article	IF	CITATIONS
163	Confinement of poly(allylamine) in Preyssler-type polyoxometalate and potassium ion framework for enhanced proton conductivity. Communications Chemistry, 2019, 2, .	4.5	31
164	Infrared Study of CO Adsorption and Oxidation over Au/Al2O3Catalyst at 150 K. Journal of Physical Chemistry B, 2001, 105, 3017-3022.	2.6	30
165	Methanol-to-olefin over gallosilicate analogues of chabazite zeolite. Microporous and Mesoporous Materials, 2008, 116, 253-257.	4.4	30
166	Dinitrogen as a probe of acid sites of zeolites. Catalysis Letters, 1993, 21, 257-264.	2.6	29
167	Photoluminescence and FT-IR studies of the dissociative adsorption of H2 on the active ZrO2 catalyst and its role in the hydrogenation of CO. Research on Chemical Intermediates, 1990, 13, 195-202.	2.7	28
168	A functional mesoporous ionic crystal based on polyoxometalate. Dalton Transactions, 2016, 45, 2805-2809.	3.3	28
169	Consequences of Fe speciation in MFI zeolites for hydroxylation of benzene to phenol with H2O2. Applied Catalysis A: General, 2019, 579, 159-167.	4.3	28
170	Isotope-exchange reaction between hydrogen molecules and surface hydroxy groups on bare and modified ZrO2. Journal of the Chemical Society, Faraday Transactions, 1996, 92, 4491.	1.7	27
171	Synthesis of Highly Ordered Mesoporous Tantalum Oxide. Chemistry Letters, 2005, 34, 394-395.	1.3	27
172	Effect of Pt nanoparticle decoration on the H2 storage performance of plasma-derived nanoporous graphene. Carbon, 2021, 171, 294-305.	10.3	27
173	IRAS and TPD study of adsorbed formic acid on Pt(110)-(1 × 2) surface. Surface Science, 1996, 368, 270-274.	1.9	26
174	Double bond migration of 1-butene without protonated intermediate on D-ZSM-5. Microporous and Mesoporous Materials, 1998, 21, 429-437.	4.4	26
175	Pronounced Selectivity in Matrix-Assisted Laser Desorptionâ^'lonization Mass Spectrometry with 2,4,6-Trihydroxyacetophenone on a Zeolite Surface: Intensity Enhancement of Protonated Peptides and Suppression of Matrix-Related Ions. Journal of Physical Chemistry C, 2010, 114, 1593-1600.	3.1	26
176	Mechano-catalytic overall water splitting on some oxides (II). Applied Catalysis A: General, 2000, 200, 255-262.	4.3	25
177	Preparation and Photocatalysis of Ordered Mesoporous Mg-Ta Mixed Oxide. Chemistry Letters, 2002, 31, 498-499.	1.3	25
178	Regiocontrolled Oxidative Coupling Polycondensation of 2,5-Dimethylphenol Induced by Mesoporous Interior. Macromolecules, 2004, 37, 9657-9659.	4.8	25
179	Triblock copolymer-assisted synthesis of a hybrid mesoporous ethenylene–silica with 2D hexagonal structure and large pores. Journal of Materials Chemistry, 2005, 15, 2362.	6.7	25
180	Preparation of Chiral Mesoporous Materials with Helicity Perfectly Controlled. Chemistry of Materials, 2011, 23, 2014-2016.	6.7	25

#	Article	IF	CITATIONS
181	Measurement of vibrational energy relaxation of a surface hydroxyl group by ultrashort tunable infrared pulses. Surface Science, 1993, 283, 244-247.	1.9	24
182	IR study on H/D isotope exchange reactions of formate and methoxy species with D2 on ZrO2. Journal of the Chemical Society, Faraday Transactions, 1997, 93, 169-174.	1.7	24
183	Supermicroporous Niobium Oxide as an Acid Catalyst. Catalysis Letters, 2004, 98, 181-186.	2.6	24
184	In Situ TEM Observation of Crystallization of Amorphous Ordered Mesoporous Nbâ^'Ta and Mgâ^'Ta Mixed Oxides. Chemistry of Materials, 2005, 17, 632-637.	6.7	24
185	Changes in Surface Property and Catalysis of Mesoporous Nb2O5 from Amorphous to Crystalline Pore Walls. Catalysis Letters, 2011, 141, 283-292.	2.6	24
186	Mechanism of Decomposition of Surface Ethoxy Species to Ethene and Acidic OH Groups on H-ZSM-5. Journal of Physical Chemistry Letters, 2015, 6, 2243-2246.	4.6	24
187	An attempt to a semi-quantitative analysis of Lewis acid sites in H-ZSM-5 zeolite using water as an IR-spectroscopic titrant. Catalysis Letters, 1996, 38, 15-19.	2.6	23
188	In Situ Observation of the Dehydration of Formate on Ni(110). Journal of Physical Chemistry B, 1997, 101, 5177-5181.	2.6	23
189	IRAS study of π-bonded ethylene on a Pt(111) surface in the presence of gaseous ethylene and hydrogen. Applied Surface Science, 1997, 121-122, 548-551.	6.1	23
190	Vibrational Study of Layered Perovskites M2La2Ti3O10(M = Li, Na, K, Rb):Â Raman Spectra and Normal Mode Analysis. Journal of Physical Chemistry B, 2001, 105, 7950-7953.	2.6	23
191	Synthesis of crystallized mesoporous transition metal oxides by silicone treatment of the oxide precursor. Chemical Communications, 2006, , 2188.	4.1	23
192	Vibrational lifetimes of surface hydroxyl groups of zeolites by picosecond IR pulses. Chemical Physics Letters, 1993, 204, 273-276.	2.6	22
193	Synthesis and Property of Mesoporous Tantalum Oxides. Topics in Catalysis, 2002, 19, 171-177.	2.8	22
194	Infrared studies of ethene hydrogenation over ZrO2. Part 1.—Ethene adsorption. Journal of the Chemical Society, Faraday Transactions, 1990, 86, 3021-3026.	1.7	21
195	The effect of adsorbed noble gas atoms on vibrational relaxation of hydroxyl group in zeolite. Journal of Chemical Physics, 1996, 105, 279-288.	3.0	21
196	IR study on migration of 18OCH3 species on ZrO2. Catalysis Letters, 1998, 50, 179-181.	2.6	21
197	Novel methods for preparation of ion-exchangeable thin films. Thin Solid Films, 1999, 343-344, 156-159.	1.8	20
198	Ultra-fine Tuning of Microporous Opening Size in Zeolite by CVD. Journal of Physical Chemistry B, 2004, 108, 2295-2299.	2.6	20

#	Article	IF	CITATIONS
199	Synthesis, characterization and catalytic studies of CHA zeotype materials containing boron and iron. Catalysis Communications, 2009, 10, 447-450.	3.3	20
200	Infrared studies of ethene hydrogenation over ZrO2. Catalysis Letters, 1992, 12, 127-137.	2.6	19
201	Crystallization of an Ordered Mesoporous Nb–Ta Oxide. Angewandte Chemie, 2003, 115, 2484-2487.	2.0	19
202	Cs-Beta with an Al-rich composition as a highly active base catalyst for Knoevenagel condensation. Applied Catalysis A: General, 2019, 575, 20-24.	4.3	19
203	Hydroconversion of methyl laurate over beta-zeolite-supported Ni–Mo catalysts: Effect of acid and base treatments of beta zeolite. Fuel Processing Technology, 2020, 197, 106182.	7.2	19
204	CHA-Type Zeolite Prepared by Interzeolite Conversion Method Using FAU and LTL-Type Zeolite: Effect of the Raw Materials on the Crystallization Mechanism, and Physicochemical and Catalytic Properties. Catalysts, 2020, 10, 1204.	3.5	19
205	Infrared studies of methanol adsorbed on magnesium oxide. Applied Surface Science, 1987, 28, 475-478.	6.1	18
206	CO coadsorption-induced recombination of surface hydroxyls to water on Ni(110) surface by IRAS and TPD. Surface Science, 1995, 325, 223-229.	1.9	18
207	Suppression of formation of ethylidyne on Pt(111) by reversibly adsorbed di-σ-bonded ethylene studied by in situ IRAS. Surface Science, 1998, 415, L983-L987.	1.9	18
208	Adsorption Structures of Carbon Dioxide on NiO(111) and Hydroxylated NiO(111) Studied by Infrared Reflection Adsorption Spectroscopy. Langmuir, 1999, 15, 2158-2161.	3.5	18
209	Synthesis of Sn-containing mesoporous silica nanospheres as efficient catalyst for Baeyer–Villiger oxidation. Applied Catalysis A: General, 2015, 490, 93-100.	4.3	18
210	Infrared studies of ethene hydrogenation over ZrO2. Part 3.—Reaction mechanism. Journal of the Chemical Society, Faraday Transactions, 1992, 88, 2095-2099.	1.7	17
211	An IRAS study of hydroxyl species (OD(a)) on oxygen-modified Cu(110) surface. Surface Science, 1993, 295, 169-173.	1.9	17
212	Isotope Exchange Reaction of Formate with Molecular Hydrogen on Ni(110) by IRAS. The Journal of Physical Chemistry, 1996, 100, 18177-18182.	2.9	17
213	Thermal Conversion of Methoxy Species on Dimethyl Ether Adsorbed CeO2. The Journal of Physical Chemistry, 1996, 100, 14462-14467.	2.9	17
214	A Novel Route of Double-Bond Migration of an Olefin without Protonated Species on ZSM-5 Zeolite. Journal of Physical Chemistry B, 1997, 101, 5477-5479.	2.6	17
215	Direct Observation of Surface Intermediates Formed by Selective Oxidation of Alcohols on Silica-Supported Molybdenum Oxide. Journal of Physical Chemistry B, 2004, 108, 3231-3239.	2.6	17
216	Enhanced hydrogen chemisorption and spillover on non-metallic nickel subnanoclusters. Journal of Materials Chemistry A, 2018, 6, 12523-12531.	10.3	17

#	Article	IF	CITATIONS
217	Bimetallic Fe–Cu/beta zeolite catalysts for direct hydroxylation of benzene to phenol: effect of the sequence of ion exchange for Fe and Cu cations. Catalysis Science and Technology, 2020, 10, 6977-6986.	4.1	17
218	Ion-exchangeable thin films derived from a layered titanate, Cs0.68Ti1.83â–¡0.17O4 (â–¡:vacancy). Physical Chemistry Chemical Physics, 2001, 3, 640-644.	2.8	16
219	Synthesis and application for overall water splitting of transition metal-mixed mesoporous Ta oxide. Solid State Ionics, 2002, 151, 305-311.	2.7	16
220	Standardization of catalyst preparation using reference catalyst: ion exchange of mordenite type zeolite. Applied Catalysis A: General, 2005, 283, 63-74.	4.3	16
221	Standardization of catalyst preparation using reference catalyst: ion exchange of mordenite type zeolite. Applied Catalysis A: General, 2005, 283, 75-84.	4.3	16
222	Methanol conversion to lower olefins over RHO type zeolite. Catalysis Communications, 2013, 37, 1-4.	3.3	16
223	Synergetic effect in heterogeneous acid catalysis by a porous ionic crystal based on Al( <scp>iii</scp> )–salphen and polyoxometalate. Dalton Transactions, 2017, 46, 3105-3109.	3.3	16
224	Ethanol–ethylene conversion mechanism on hydrogen boride sheets probed by <i>in situ</i> infrared absorption spectroscopy. Physical Chemistry Chemical Physics, 2021, 23, 7724-7734.	2.8	16
225	Vibrational lifetime of surface species of zeolites by picosecond IR pulses. Journal of Electron Spectroscopy and Related Phenomena, 1993, 64-65, 259-267.	1.7	15
226	An infrared study of selective hydrogenation of carboxylic acids to corresponding aldehydes over a ZrO2 catalyst: pivalic acid to 2,2-dimethylpropanal. Catalysis Letters, 1993, 17, 309-317.	2.6	15
227	Migration of butene isomers onto the acidic OH groups in small micropores of ferrierite. Catalysis Today, 2000, 63, 305-308.	4.4	15
228	Shape selective adsorption of olefins on BrÃ,nsted acidic OH (OD) groups on ferrierite studied by FT-IR. Applied Catalysis A: General, 2000, 194-195, 275-283.	4.3	15
229	Simultaneous Observation of Alkenyl Carbenium Ions and Alkoxy Species on HZSM-5 Zeolite by Adsorption of 1-Methylcyclopentene and 1-Methylcyclopentanol. Journal of Physical Chemistry B, 2001, 105, 7878-7881.	2.6	15
230	Synthesis of well-ordered nanospheres with uniform mesopores assisted by basic amino acids. Studies in Surface Science and Catalysis, 2007, 170, 1774-1780.	1.5	15
231	Direct FT-IR observation of oxidation of 1-hexene and cyclohexene with H2O2 over TS-1. Microporous and Mesoporous Materials, 2010, 135, 13-20.	4.4	15
232	Synthesis and catalytic properties of porous Nb–Mo oxide solid acid. Catalysis Today, 2011, 164, 358-363.	4.4	15
233	IR Characterization of Mesoporous Tantalum Oxide, Ta-TMS-1. Bulletin of the Chemical Society of Japan, 2000, 73, 1123-1129.	3.2	14
234	Probing the basicity of lattice oxygen on H-form zeolites using CO2. Journal of Catalysis, 2019, 371, 291-297.	6.2	14

#	Article	IF	CITATIONS
235	IRAS study of hydroxyl species on NiO/Ni(110): formation and isotope exchange reaction. Surface Science, 1995, 343, 71-79.	1.9	13
236	SFG study of formic acid on a Pt(110)-(1 × 2) surface. Surface Science, 1996, 357-358, 651-655.	1.9	13
237	Time-Resolved Sum Frequency Generation Reveals Adsorbate Migration between Different Surface Active Sites on Titanium Oxide/Pt(111). Journal of the American Chemical Society, 2009, 131, 4580-4581.	13.7	13
238	Highly efficient transformation of linear poly(phenylene ethynylene)s into zigzag-shaped ï€-conjugated microporous polymers through boron-mediated alkyne benzannulation. Materials Chemistry Frontiers, 2018, 2, 807-814.	5.9	13
239	IRAS study of adsorption and transformation of CH2I2 on Al(111) surface. Surface Science, 1996, 349, 294-300.	1.9	12
240	Rapid-scanning FT-IR study on the adsorptions of methanol and water on H-ZSM-5 zeolite. Studies in Surface Science and Catalysis, 1997, 105, 1739-1746.	1.5	12
241	Infrared Spectroscopic Study of High Temperature Behavior of the BrÃ,nsted Acidic Hydroxyl Groups on Zeolites. Bulletin of the Chemical Society of Japan, 1998, 71, 2149-2152.	3.2	12
242	Overall water splitting on Cu(l)-containing ternary oxides, CuMO2(M&dbndFe, Ga, Al) with delafossite structure. Studies in Surface Science and Catalysis, 1999, , 301-304.	1.5	12
243	Preparation of Ordered Supermicroporous Niobium Oxide. Chemistry Letters, 2002, 31, 1058-1059.	1.3	12
244	Ethene oligomerization on H-ZSM-5 in relation to ethoxy species. Catalysis Science and Technology, 2014, 4, 4193-4195.	4.1	12
245	Titanium(IV) in the Organicâ€Structureâ€Directingâ€Agentâ€Free Synthesis of Hydrophobic and Largeâ€Pore Molecular Sieves as Redox Catalysts. ChemSusChem, 2015, 8, 2476-2480.	6.8	12
246	Hydrophobicity enhancement of Ti-MWW catalyst and its improvement in oxidation activity. Applied Catalysis A: General, 2015, 503, 156-164.	4.3	12
247	Population lifetimes of the OH stretching band of water molecules on zeolite surfaces. Chemical Physics Letters, 1996, 261, 534-538.	2.6	11
248	Transient absorption spectra of vibrationally excited OH/OD groups in mordenite zeolites: Effect of Xe adsorption. Journal of Chemical Physics, 1996, 105, 6665-6672.	3.0	11
249	A microporous structure of a thin film made of an ion-exchangeable layered compound. Supramolecular Science, 1998, 5, 229-233.	0.7	11
250	FT-IR Study of H2 and H2 adsorption on H-ferrierite. Journal of Molecular Catalysis A, 1999, 137, 269-272.	4.8	11
251	Oxidative Coupling Polymerization of 2,6-Dimethylphenol with a Copper–Amine Catalyst Immobilized within the Interior of SBA-15. Chemistry Letters, 2005, 34, 662-663.	1.3	11
252	Consideration of Acid Strength of a Single OH Group on Zeolites by Isotope Exchange Reaction with Ethane at High Temperatures. Topics in Catalysis, 2017, 60, 1496-1505.	2.8	11

#	Article	IF	CITATIONS
253	Development of AEI-type boroaluminosilicate zeolites, and their acidic and catalytic properties in ethene conversion reaction. Applied Catalysis A: General, 2018, 568, 123-129.	4.3	11
254	Investigation of the acidic nature of MCM-68 zeolite based on the adsorption of CO and bulky probe molecules. Microporous and Mesoporous Materials, 2018, 272, 16-23.	4.4	11
255	Infrared studies of ethene hydrogenation over ZrO2. Part 2.—Ethane adsorption. Journal of the Chemical Society, Faraday Transactions, 1990, 86, 3665-3669.	1.7	10
256	Preparation and characteristics of crystallized mesoporous Zr6Nb2O17. Microporous and Mesoporous Materials, 2004, 75, 203-208.	4.4	10
257	lron- and Copper-exchanged Beta Zeolite Catalysts for Hydroxylation of Benzene to Phenol with H <sub>2</sub> O <sub>2</sub> . Chemistry Letters, 2018, 47, 1112-1115.	1.3	10
258	A mechanism of ethene hydrogenation over ZRO2 studied by infrared spectroscopy. Research on Chemical Intermediates, 1993, 19, 521-551.	2.7	9
259	Matrix-assisted laser desorption ionization using lithium-substituted mordenite surface. Chemical Physics Letters, 2012, 546, 159-163.	2.6	9
260	Hexamethyleneimine and pivalonitrile as location probe molecules of Lewis acid sites on MWW-type zeolites. Microporous and Mesoporous Materials, 2015, 206, 86-94.	4.4	9
261	The effective silylation of external surface on H-ZSM5 with cyclic siloxane for the catalytic cracking of naphtha. Molecular Catalysis, 2017, 433, 48-54.	2.0	9
262	Effect of the ammonium ion on proton conduction in porous ionic crystals based on Keggin-type silicododecatungstate. Acta Crystallographica Section C, Structural Chemistry, 2018, 74, 1289-1294.	0.5	9
263	Synthesis of Ga-containing CON-type material and its catalytic performance in methanol-to-olefins reaction. Catalysis Today, 2020, 352, 175-182.	4.4	9
264	Characterization of H4SiW12O40 supported on mesoporous silica (SBA-15), non-structured amorphous silica and Î <sup>3</sup> -alumina. Journal of Catalysis, 2021, 395, 387-398.	6.2	9
265	Selective synthesis of 5-hydroxymethylfurfural over natural rubber–derived carbon/silica nanocomposites with acid–base bifunctionality. Fuel, 2022, 311, 122577.	6.4	9
266	2.7 Infrared Spectroscopic Observation of N2 Species Adsorbed on BrÃ,nsted and Lewis Acid Sites of H-Zeolites at Low Temperatures. Studies in Surface Science and Catalysis, 1994, 90, 157-162.	1.5	8
267	Vibrational relaxation of hydroxyl groups in zeolite: the effect of adsorbed Xe. Surface Science, 1996, 363, 397-402.	1.9	8
268	Exchange Reaction of Adsorbed Formate with Gaseous Formic Acid on Ni(110) Studied by Time-Resolved Fourier Transform Infrared Reflection Absorption Spectroscopy. Journal of Physical Chemistry B, 1998, 102, 4401-4403.	2.6	8
269	Photocatalytic water decomposition by layered perovskites. Studies in Surface Science and Catalysis, 2000, , 1943-1948.	1.5	8
270	Conduction and Valence Band Positions of Ta2O5, TaON, and Ta3N5 by UPS and Electrochemical Methods ChemInform, 2003, 34, no.	0.0	8

#	Article	IF	CITATIONS
271	Spectroscopic Study of H2 and CO Adsorption on Platinum-Promoted Sulfated Zirconia Catalysts. Journal of Physical Chemistry B, 2003, 107, 11951-11959.	2.6	8
272	Effect of post-calcination thermal treatment on acid properties and pores structure of a mesoporous niobium–tungsten oxide. Catalysis Today, 2012, 192, 144-148.	4.4	8
273	Identification of the Basic Sites on Nitrogen-Substituted Microporous and Mesoporous Silicate Frameworks Using CO <sub>2</sub> as a Probe Molecule. Langmuir, 2018, 34, 1376-1385.	3.5	8
274	Thin (single–triple) niobium oxide layers on mesoporous silica substrate. Microporous and Mesoporous Materials, 2018, 262, 191-198.	4.4	8
275	Methanolâ€toâ€Olefins Reaction over Largeâ€Pore Zeolites: Impact of Pore Structure on Catalytic Performance. Chemie-Ingenieur-Technik, 2021, 93, 990-1000.	0.8	8
276	Synthesis of novel aluminoborosilicate isomorphous to zeolite TUN and its acidic and catalytic properties. Microporous and Mesoporous Materials, 2021, 323, 111237.	4.4	8
277	An IRAS study of adsorbed acrylonitrile on Cu(110) surface. Journal of Electron Spectroscopy and Related Phenomena, 1993, 64-65, 137-144.	1.7	7
278	Formation of stable alkenyl carbenium ions in high yield by adsorption of 1-methylcyclopentene on zeolite Y at low temperature. Chemical Communications, 2001, , 2008-2009.	4.1	7
279	Adsorption, Migration and Reactions of Hydrocarbons on Zeolites Observed by Ftir Spectroscopy. Catalysis Surveys From Asia, 2002, 5, 139-149.	1.2	7
280	The effect of main chain length of 2-methylalkane on adsorption onto OH in the micropores of zeolite. Physical Chemistry Chemical Physics, 2003, 5, 3306.	2.8	7
281	Probing the Locations of Ag+and Hydroxy Groups in AgA Zeolites by in situ FTIR Spectroscopy. Chemistry Letters, 2003, 32, 792-793.	1.3	7
282	Intramolecular H/D Exchange of Ethanol Catalyzed by Acidic OH Groups on H-ZSM-5 Zeolite. Journal of Physical Chemistry Letters, 2014, 5, 3528-3531.	4.6	7
283	One-pot synthesis of highly active Fe-containing MWW zeolite catalyst: Elucidation of Fe species and its impact on catalytic performance. Advanced Powder Technology, 2021, 32, 1070-1080.	4.1	7
284	Preparation of SiO2-pillared layered titanate thin films. Journal of Materials Research, 2000, 15, 2587-2590.	2.6	6
285	Spillover and Migration of Alkoxy Groups Formed by Adsorption of Alcohols on Silica-supported Molybdenum Oxide. Chemistry Letters, 2002, 31, 1082-1083.	1.3	6
286	Preparation and Catalytic Application of Transition Metal (Fe, V, or Cu) Oxides Homogeneously Dispersed in the Wall of Mesoporous Nb2O5. Chemistry Letters, 2003, 32, 1034-1035.	1.3	6
287	Characterization of Ag+-Exchanged Zeolite A with H2and CO Adsorption by FTIR. Bulletin of the Chemical Society of Japan, 2004, 77, 1627-1634.	3.2	6
288	Direct Observation of Unstable Intermediate Species in the Reaction oftrans-2-Butene on Ferrierite Zeolite by Picosecond Infrared Laser Spectroscopy. Journal of Physical Chemistry B, 2005, 109, 17217-17223.	2.6	6

#	Article	IF	CITATIONS
289	Systematical investigation on characteristics of a photocatalyst: tantalum oxynitrides. Microscopy (Oxford, England), 2014, 63, 313-324.	1.5	6
290	Insight into the crystallization mechanism of the CON-type zeolite. Microporous and Mesoporous Materials, 2020, 302, 110213.	4.4	6
291	Versatile phosphorus-structure-directing agent for direct preparation of novel metallosilicate zeolites with IFW-topology. Microporous and Mesoporous Materials, 2021, 317, 111005.	4.4	6
292	Surfactant-Assisted Direct Crystallization of CON-Type Zeolites with Particle Size and Acid-Site Location Controlled. Industrial & amp; Engineering Chemistry Research, 2022, 61, 1733-1747.	3.7	6
293	Dinitrogen Species Adsorbed on ZrO2Studied by Infrared Spectroscopy. Chemistry Letters, 1989, 18, 711-714.	1.3	5
294	Exchange reaction of formate with gas-phase acetic acid on Ni(110). Surface Science, 1999, 433-435, 210-214.	1.9	5
295	Oxidative Coupling Polymerization of Substituted Phenols with a Copper Amine Catalyst Immobilized within Mesoporous Silica. Macromolecular Symposia, 2006, 245-246, 87-92.	0.7	5
296	Sum Frequency Generation Spectroscopic Investigation of TiO <sub><i>x</i></sub> /Pt(111): Surface Active Sites and Reaction Paths Probed by Formate. Journal of Physical Chemistry C, 2008, 112, 12477-12485.	3.1	5
297	Biphasic Polycondensation of 4-Bromo-2,6-dimethylphenol Using Silica Gel as a Promoter. Polymer Journal, 2009, 41, 63-68.	2.7	5
298	Mechanisms of reactions of methoxy species with benzene and cyclohexane over H-ZSM-5 zeolites. Catalysis Science and Technology, 2015, 5, 3598-3602.	4.1	5
299	Monolayer Tantalum Oxide on Mesoporous Silica Substrate. ChemistrySelect, 2016, 1, 3124-3131.	1.5	5
300	Crystallization of Ti-Rich *BEA Zeolites by the Combined Strategy of Using Ti–Si Mixed Oxide Composites and Intentional Aluminum Addition/Post-Synthesis Dealumination. Crystal Growth and Design, 2018, 18, 2180-2188.	3.0	5
301	IR observation of activated ether species on acidic OH groups on H-ZSM-5 zeolites. Molecular Catalysis, 2019, 477, 110535.	2.0	5
302	Development of mesopore-containing CON-type zeolite with unique acidic and catalytic properties. Catalysis Science and Technology, 2020, 10, 4293-4304.	4.1	5
303	Fabrication of AEI-type aluminosilicate catalyst with sheet-like morphology for direct conversion of propene to butenes. Catalysis Science and Technology, 2021, 11, 5839-5848.	4.1	5
304	FT-IR studies of decarbonylation and recarbonylation of [Pt3(CO)6] 5 2? supported on dehydrated SiO2. Catalysis Letters, 1996, 40, 81-87.	2.6	4
305	Reversible photodissociation of Mo(CO)6 in a zeolite cage. Catalysis Letters, 1996, 40, 89-94.	2.6	4
306	Comments on "N2Adsorption at 77 K on H-Mordenite and Alkali-Metal-Exchanged Mordenites: An IR Study― The Journal of Physical Chemistry, 1996, 100, 18882-18882.	2.9	4

#	Article	IF	CITATIONS
307	Unusual isomerization routes of n-butenes on the acidic OH (OD) groups on ferrierite zeolite studied by FT-IR. Studies in Surface Science and Catalysis, 2000, , 2933-2938.	1.5	4
308	Single crystal particles of mesoporous (Nb, Ta)2O5. Studies in Surface Science and Catalysis, 2002, 141, 265-272.	1.5	4
309	Oxysulfides Ln2Ti2S2O5 as Stable Photocatalysts for Water Oxidation and Reduction under Visible-Light Irradiation ChemInform, 2004, 35, no.	0.0	4
310	Control of Pore Size in Mesoporous Silica by Incremental Surface Modification Using Tetramethyl Orthosilicate. Chemistry Letters, 2005, 34, 596-597.	1.3	4
311	Effect of the preparation conditions of a barium–tantalate photocatalyst on the overall photocatalytic splitting of H2O. Catalysis Science and Technology, 2013, 3, 1691.	4.1	4
312	Co-reaction of methanol and ethylene over MFI and CHA zeolitic catalysts. Microporous and Mesoporous Materials, 2018, 255, 174-184.	4.4	4
313	Reaction-probe infrared investigation on drastic change in reactivity of mesoporous silica for acetalization of cyclohexanone with methanol; pore-size dependence. Microporous and Mesoporous Materials, 2019, 278, 91-98.	4.4	4
314	Highly thermostable high molecular-weight low k PIM polymers based on 5,5′,6,6′-tetrahydroxy-3,3,3′,3′-Tetramethylspirobisindane, decafluorobiphenyl, and bisphenols. Polym 2021, 230, 124072.	eß.8	4
315	Infrared Studies of Ethene Hydrogenation over ZrO2. Journal of Electron Spectroscopy and Related Phenomena, 1990, 54-55, 805-814.	1.7	3
316	IR observation of adsorption and initial reactions of olefins on BrÃ,nsted acid sites of a deuterated ZSM-5. Research on Chemical Intermediates, 1998, 24, 411-423.	2.7	3
317	In situ observation of the exchange reaction of formate with molecular formic acid on Ni(110). Journal of Molecular Catalysis A, 1999, 141, 73-82.	4.8	3
318	Evaluation of Ti Distribution in Zeolite Framework Based on the Catalytic Activity for Alkene Epoxidation. Chemistry Letters, 2019, 48, 1130-1133.	1.3	3
319	Ultrafast Encapsulation of Metal Nanoclusters into MFI Zeolite in the Course of Its Crystallization: Catalytic Application for Propane Dehydrogenation. Angewandte Chemie, 2020, 132, 19837-19842.	2.0	3
320	Mechano-catalytic overall water-splitting into hydrogen and oxygen on some metal oxides. , 2000, , 159-179.		3
321	Characterization of Layered Titanate Thin Films. Electrochemistry, 1999, 67, 1224-1226.	1.4	3
322	Does the IR spectroscopic result of 14N15N adsorption on H-form zeolites mean the side-on type adsorption of the N2 species?. Microporous Materials, 1993, 2, 35-39.	1.6	2
323	Hydrogen adsorption and spillover on Ru/ZrO2. Studies in Surface Science and Catalysis, 1997, , 73-80.	1.5	2
324	Migration of Methyl Species of Surface Methoxy Groups on Ta-TMS1. Chemistry Letters, 1998, 27, 869-870.	1.3	2

#	Article	IF	CITATIONS
325	Layered titanate thin film as an electrode material. Journal of Materials Research, 2004, 19, 661-666.	2.6	2
326	Sulfonated Incompletely Carbonized Glucose as Strong BrÃ,nsted Acid Catalyst. Studies in Surface Science and Catalysis, 2007, 172, 405-408.	1.5	2
327	Surface properties of Ta2O5 layers prepared on SBA-15. Catalysis Today, 2012, 192, 197-202.	4.4	2
328	Synthesis of SFH-type aluminosilicate zeolite with 14-membered ring and its applications as solid acidic catalyst. Microporous and Mesoporous Materials, 2014, 193, 166-172.	4.4	2
329	Estimation of the real temperature of samples in IR cell using OH frequency of silica. Surface and Interface Analysis, 2015, 47, 166-168.	1.8	2
330	Photocatalytic property of strontium–niobium mixed oxide prepared by utilizing organic mediators to the overall splitting of H2O. Catalysis Today, 2015, 246, 172-175.	4.4	2
331	Desorption of Dimethyl Ether from a Methoxy Species Formed on a CeO2Surface. Langmuir, 1996, 12, 6712-6713.	3.5	1
332	Reply to Comment on "Thermal Conversion of Methoxy Species on Dimethyl Ether Adsorbed CeO2― Journal of Physical Chemistry B, 1997, 101, 1486-1487.	2.6	1
333	IR Observation of Hydrogen Adsorption on Active and Inactive Pt/SO42â^–ZrO2. Chemistry Letters, 2003, 32, 408-409.	1.3	1
334	Novel Synthesis and Photocatalytic Activity of Oxysulfide Sm2Ti2S2O5 ChemInform, 2004, 35, no.	0.0	1
335	Preparation of crack-free, transparent, nanoporous niobium oxide film with crystalline structure by evaporation-induced self-assembly (EISA) process. Studies in Surface Science and Catalysis, 2005, , 321-326.	1.5	1
336	Photoinduced Transformation of Silicone-modified TiO2. Chemistry Letters, 2005, 34, 198-199.	1.3	1
337	Highly pH-dependent Facile-preparation of Amorphous High Surface Area Aluminum Hydroxide-bicarbonates with [ε-Al <sub>13</sub> O <sub>4</sub> (OH) <sub>24</sub> (H <sub>2</sub> O) <sub>12</sub> ] <sup>7+</sup> . Chemistry Letters, 2018, 47, 668-670.	1.3	1
338	MALDI Mass Spectrometry of Small Molecules Using Nanometer-sized Clay. Analytical Sciences, 2020, 36, 177-181.	1.6	1
339	In-situ far-infrared study of vibrations between zeolite frameworks and metallic or molecular cations. Microporous and Mesoporous Materials, 2020, 305, 110345.	4.4	1
340	Homogeneous Chemical Functionalization of the Mesoporous Silica Interior and the Utilization as the Polymerization Sites. Yuki Gosei Kagaku Kyokaishi/Journal of Synthetic Organic Chemistry, 2008, 66, 1187-1198.	0.1	1
341	<title>Infrared-visible sum frequency generation spectroscopy applied to adsorption and reaction at solid surfaces</title> . , 1995, 2547, 12.		0
342	TiNxOyFz as a Stable Photocatalyst for Water Oxidation in Visible Light (< 570 nm) ChemInform, 2003, 34, no.	0.0	0

#	Article	IF	CITATIONS
343	Formation and Desorption of Oxygen Species in Nanoporous Crystal 12CaO×7Al2O3 ChemInform, 2004, 35, no.	0.0	0
344	Porous Single-Crystalline TaON and Ta3N5 Particles ChemInform, 2004, 35, no.	0.0	0
345	Electrochemical Behavior of Thin Ta3N5 Semiconductor Film ChemInform, 2004, 35, no.	0.0	0
346	Kinetic Study of Dehydrogenation between H–Siloxane and Ti–OH on TiO2. Chemistry Letters, 2005, 34, 460-461.	1.3	0
347	Exfoliated HNb3O8 Nanosheets as a Strong Protonic Solid Acid ChemInform, 2005, 36, no.	0.0	0
348	Photocatalytic Decomposition of Water by a Novel Photocatalyst, Ge3N4. Studies in Surface Science and Catalysis, 2007, 172, 433-436.	1.5	0
349	Synthesis of NaNbO3 under non-hydrothermal conditions from sodium niobate precursors prepared by alkaline treatment of amorphous Nb2O5. Journal of Solid State Chemistry, 2021, 295, 121891.	2.9	0
350	Infrared studies of direct production of benzaldehyde from benzoic acid and H2 over a modified ZrO2. , 1994, , 99-102.		0